

# CONTROLLING PROPAGATION OF EPIDEMICS VIA MEAN-FIELD GAMES

WONJUN LEE, SITING LIU, HAMIDOU TEMBINE, WUCHEN LI, AND STANLEY OSHER

**ABSTRACT.** The coronavirus disease 2019 (COVID-19) pandemic is changing and impacting lives on a global scale. In this paper, we introduce a mean-field game model in controlling the propagation of epidemics on a spatial domain. The control variable, the spatial velocity, is first introduced for the classical disease models, such as the SIR model. For this proposed model, we provide fast numerical algorithms based on proximal primal-dual methods. Numerical experiments demonstrate that the proposed model illustrates how to separate infected patients in a spatial domain effectively.

## 1. INTRODUCTION

The outbreak of COVID-19 epidemic has resulted in over millions of confirmed cases and hundred thousands of deaths globally. It has a huge impact on global economy as well as everyone's daily life. There has been a lot of interest in modeling the dynamics and propagation of the epidemic. One of the well-known and basic models in epidemiology is the SIR model proposed by Kermack and McKendrick [25] in 1927. Here, S, I, R represent the number of susceptible, infected and recovered people respectively. They use an ODE system to describe the transmission dynamics of infectious diseases among the population. As the propagation of COVID-19 has significant spatial characteristic, actions such as travel restrictions, physical distancing and self-quarantine are taken to slow down the spread of the epidemic. It is important to have a spatial-type SIR model to study the spread of the infectious disease and movement of individuals [24, 23, 17].

Since the epidemic has affected the society and individuals significantly, mean-field games (MFG) provide a perspective to study and understand the underlying population dynamics. Mean-field games were introduced by Jovanovic and Rosenthal [22], Huang, Malhamé, and Caines [18], and Lasry and Lions [28, 29]. They model a huge population of agents playing dynamic games. There is growing research interest in this direction. For a review of MFG theory, we refer to [30, 14]. With wide application to various fields [15, 6, 26, 1], computational methods are also designed to solve related high dimensional MFG problems [3, 5, 12, 32, 36, 33].

In this paper, we combine the above ideas of spatial SIR model and MFG. In other words, we introduce a mean-field game (control) model for controlling the virus spreading within a spatial domain. Here the goal is to minimize the number of infectious agents and the amount of movement of the population. In short, we formalize the following

---

This work is supported by AFOSR MURI FA9550-18-1-0502.

constrained optimization problem

$$\inf_{(\rho_i, v_i)_{i \in \{S, I, R\}}} E(\rho_I(T, \cdot)) + \int_0^T \int_{\Omega} \sum_{i \in \{S, I, R\}} \frac{\alpha_i}{2} \rho_i \|v_i\|^2 + \frac{c}{2} (\rho_S + \rho_I + \rho_R)^2 dx dt$$

subject to

$$\begin{cases} \partial_t \rho_S + \nabla \cdot (\rho_S v_S) + \beta \rho_S \rho_I - \frac{\eta_S^2}{2} \Delta \rho_S = 0 \\ \partial_t \rho_I + \nabla \cdot (\rho_I v_I) - \beta \rho_S \rho_I + \gamma \rho_I - \frac{\eta_I^2}{2} \Delta \rho_I = 0 \\ \partial_t \rho_R + \nabla \cdot (\rho_R v_R) - \gamma \rho_I - \frac{\eta_R^2}{2} \Delta \rho_R = 0 \\ \rho_S(0, \cdot), \rho_I(0, \cdot), \rho_R(0, \cdot) \text{ are given.} \end{cases}$$

Here  $\rho_i$  represents population density and  $v_i$  describes the movement, with  $i \in \{S, I, R\}$  corresponding to the susceptible, infected and recovered compartmental state or class. We consider the spatial SIR model with nonlocal spreading modeled by an integration kernel  $K$  representing the physical distancing and a spatial diffusion of population, and set it as dynamic to our mean-field game problem, which is the constraint to the minimization problem. Due to the multiplicative nature of the interaction term between susceptible and infectious agents  $\beta \rho_S \rho_I$ , the mean-field game problem is a non-convex problem. With Lagrange multipliers, we formalize the mean-field game problem as an unconstrained optimization problem. Fast numerical algorithms are designed to solve the non-convex optimization problem in  $2D$  with  $G - prox$  preconditioning [19].

In the literature, spatial SIR models in the form of a nonlinear integro-differential [2, 11, 38] and reaction-diffusion system [23, 17] have been studied. Traveling waves are studied to understand the propagation of various type of epidemics, such as Lyme disease, measles etc, and recently, COVID-19 [7, 16, 39, 4]. In [4], they introduce a SIRT model to study the effects of the presence of a road on the spatial propagation of the epidemic. For surveys, see [34, 35]. As for numerical modelling of epidemic model concerning spatial effect, finite-difference methods are used to discretize the reaction-diffusion system and solve the spatial SIR model and its various extensions [10, 20, 13]. Epidemic models have been treated using optimal control theory, with major control measures on medicare (vaccination) [37, 27, 21]. In [21], a feedback control problem of SIR model is studied to help determine the vaccine policy, with the goal to minimize the number of infected people. In [31], they introduce a nonlinear SIQS epidemic model on complex networks and study the optimal quarantine control. Compared to previous works, our model is the first to consider an optimal control problem for SIR on a spatial domain. In particular, we formulate velocity fields among S, I, R, populations as control variables.

Our paper is organized as follows. In section 2, we introduce the mean field control model for propagation of epidemics. We introduce a primal-dual hybrid gradient algorithm for this model in section 3. In section 4, several numerical examples are demonstrated.

## 2. MODEL

In this section, we briefly review the classical epidemics models, e.g. SIR dynamics. We then introduce a mean field control model for SIR dynamics on a spatial domain. We derive a system to find the minimizer of the proposed model.

**2.1. Review.** We first review the classical SIR model.

$$\begin{cases} \frac{dS}{dt} = -\beta SI \\ \frac{dI}{dt} = \beta SI - \gamma I \\ \frac{dR}{dt} = \gamma I \end{cases}$$

where  $S, I, R : [0, T] \rightarrow [0, 1]$  represent the proportion of the susceptible population, infected population, and recovered population, respectively, given time  $t$ . The nonnegative constants  $\beta$  and  $\gamma$  represent the rates of susceptible becoming infected and infected becoming recovered. SIR has an interpretation in terms of stochastic processes of agent-based models. The SIR model can be obtained as a motion of the law of a three-state Markov chain with the transition from  $S$  to  $I$  and  $I$  to  $R$ .

**2.2. Spatial SIR variational problem.** We then consider the spatial dimension of the  $S, I, R$  functions. Let  $\Omega \subset \mathbb{R}^d$  be a bounded domain. Consider the following functions

$$\rho_S, \rho_I, \rho_R : [0, T] \times \Omega \rightarrow \mathbb{R}_+, \quad (i \in \{S, I, R\})$$

Here,  $\rho_S, \rho_I$ , and  $\rho_R$  represent susceptible, infected, and recovered populations, respectively. We assume  $\rho_i$  for each  $i \in \{S, I, R\}$  moves on a spatial domain with velocities  $v_i$ . We can describe these movements by continuity equations.

$$\begin{cases} \partial_t \rho_S + \nabla \cdot (\rho_S v_S) + \beta \rho_S \rho_I - \frac{\eta_S^2}{2} \Delta \rho_S = 0 \\ \partial_t \rho_I + \nabla \cdot (\rho_I v_I) - \beta \rho_S \rho_I + \gamma \rho_I - \frac{\eta_I^2}{2} \Delta \rho_I = 0 \\ \partial_t \rho_R + \nabla \cdot (\rho_R v_R) - \gamma \rho_I - \frac{\eta_R^2}{2} \Delta \rho_R = 0 \\ \rho_S(0, \cdot), \rho_I(0, \cdot), \rho_R(0, \cdot) \text{ are given.} \end{cases} \quad (1)$$

where  $v_i : [0, T] \times \Omega \rightarrow \mathbb{R}^d$  ( $i \in \{S, I, R\}$ ) are vector fields that represent the velocity fields for  $\rho_i$  ( $i \in \{S, I, R\}$ ) and nonnegative constants  $\eta_i$  ( $i \in \{S, I, R\}$ ) are coefficients representing for viscosity terms. In addition, we will assume zero flux conditions by the Neumann boundary conditions. These systems of continuity equations satisfy the following equality:

$$\frac{\partial}{\partial t} \int_{\Omega} \rho_S(t, x) + \rho_I(t, x) + \rho_R(t, x) dx = 0,$$

i.e., the total mass of the populations will be conserved for all time.

Lastly, we introduce the proposed mean field control models. Consider the following variational problem:

$$\inf_{(\rho_i, v_i)_{i \in \{S, I, R\}}} E(\rho_I(T, \cdot)) + \int_0^T \int_{\Omega} \sum_{i \in \{S, I, R\}} \frac{\alpha_i}{2} \rho_i \|v_i\|^2 + \frac{c}{2} (\rho_S + \rho_I + \rho_R)^2 dxdt \quad (2)$$

subject to (1) with fixed initial densities.

Here  $E$  is a convex functional and  $\alpha_i$  ( $i \in \{S, I, R\}$ ) and  $c$  are nonnegative constants. The minimizers of the above variational problem will provide the optimal movements for each population while minimizing the terminal cost functional with respect to the infected population  $\rho_I$ . The last term in the running cost,  $\frac{c}{2}(\rho_S + \rho_I + \rho_R)^2$ , penalizes congestion of the total population.

We note that the function  $(\rho_i, v_i) \mapsto \rho_i \|v_i\|^2$  is not convex. By introducing new variables  $m_i := \rho_i v_i$ , we convert the cost function to be convex.

$$\min_{\rho_i, m_i} P(\rho_i, m_i)_{i \in \{S, I, R\}} \quad (3a)$$

subject to

$$\begin{cases} \partial_t \rho_S + \nabla \cdot m_S + \beta \rho_S \rho_I - \frac{\eta_S^2}{2} \Delta \rho_S = 0 \\ \partial_t \rho_I + \nabla \cdot m_I - \beta \rho_S \rho_I + \gamma \rho_I - \frac{\eta_I^2}{2} \Delta \rho_I = 0 \\ \partial_t \rho_R + \nabla \cdot m_R - \gamma \rho_I - \frac{\eta_R^2}{2} \Delta \rho_R = 0 \\ \rho_S(0, \cdot), \rho_I(0, \cdot), \rho_R(0, \cdot) \text{ are given.} \end{cases} \quad (3b)$$

Here

$$\begin{aligned} P(\rho_i, m_i)_{i \in \{S, I, R\}} &= E(\rho_I(T, \cdot)) + \int_0^T \int_{\Omega} F(\rho_i, m_i)_{i \in \{S, I, R\}} dxdt \\ F(\rho_i, m_i)_{i \in \{S, I, R\}} &= \frac{\alpha_S \|m_S\|^2}{2\rho_S} + \frac{\alpha_I \|m_I\|^2}{2\rho_I} + \frac{\alpha_R \|m_R\|^2}{2\rho_R} + \frac{c}{2} (\rho_S + \rho_I + \rho_R)^2. \end{aligned}$$

From an optimization viewpoint, we note that the minimization problem is not a convex problem since the coupling terms,  $\beta \rho_S \rho_I$ , in constraints make the feasible set nonconvex. To regularize the nonconvex coupling term  $\beta \rho_S \rho_I$ , we replace products by convolutions.

$$\min_{(\rho_i, v_i)_{i \in \{S, I, R\}}} P(\rho_i, m_i)_{i \in \{S, I, R\}} \quad (4a)$$

subject to

$$\begin{cases} \partial_t \rho_S(t, x) + \nabla \cdot m_S(t, x) + \beta \rho_S(t, x) \int_{\Omega} K(x, y) \rho_I(t, y) dy - \frac{\eta_S^2}{2} \Delta \rho_S(t, x) = 0 \\ \partial_t \rho_I(t, x) + \nabla \cdot m_I(t, x) - \beta \rho_I(t, x) \int_{\Omega} K(x, y) \rho_S(t, y) dy + \gamma \rho_I(t, x) - \frac{\eta_I^2}{2} \Delta \rho_I(t, x) = 0 \\ \partial_t \rho_R(t, x) + \nabla \cdot m_R(t, x) - \gamma \rho_I(t, x) - \frac{\eta_R^2}{2} \Delta \rho_R(t, x) = 0 \\ \rho_S(0, \cdot), \rho_I(0, \cdot), \rho_R(0, \cdot) \text{ given.} \end{cases} \quad (4b)$$

Here  $K(x, y)$  is a symmetric positive definite kernel representing the physical distancing between a susceptible agent located at position  $x$  and infectious agent at position  $y$ , and  $\int_{\Omega} K(x, y)\rho_I(t, y)dy$  is the exposure of a susceptible located at  $x$  to infectious agents. In this paper, we focus on a Gaussian kernel

$$K(x, y) = \frac{1}{\sqrt{(2\pi)^d}} \prod_{k=1}^d \frac{1}{\sigma_k} \exp\left(-\frac{|x_k - y_k|^2}{2\sigma_k^2}\right).$$

In modeling, the variance  $\sigma$  of Gaussian kernel can be viewed as a parameter for modeling the spatial spreading effect of virus.

*Remark 1.* The formulation is not limited to the SIR model we chose in this paper. It can be used to solve any types of spatial epidemiological models.

**2.3. Properties.** We next derive the mean field game system, i.e. the minimizer system associated with spatial SIR variational problem (4).

Define the Lagrangian functional

$$\begin{aligned} & \mathcal{L}((\rho_i, m_i, \phi_i)_{i \in \{S, I, R\}}) \\ &= P((\rho_i, m_i)_{i \in \{S, I, R\}}) - \int_0^T \int_{\Omega} \sum_{i \in \{S, I, R\}} \phi_i \left( \partial_t \rho_i + \nabla \cdot m_i - \frac{\eta_i^2}{2} \Delta \rho_i \right) dxdt \\ &+ \int_0^T \int_{\Omega} \beta \phi_I \rho_I K * \rho_S - \beta \phi_S \rho_S K * \rho_I + \gamma \rho_I (\phi_R - \phi_I) dxdt. \end{aligned} \quad (5)$$

Using this Lagrangian functional, we convert the minimization problem into a saddle problem.

$$\inf_{(\rho_i, m_i)_{i \in \{S, I, R\}}} \sup_{(\phi_i)_{i \in \{S, I, R\}}} \mathcal{L}((\rho_i, m_i, \phi_i)_{i \in \{S, I, R\}}). \quad (6)$$

Because of the nonconvex functional  $(\rho_S, \rho_I) \mapsto \rho_S \rho_I$ , the feasible set here is nonconvex. Thus, we cannot guarantee that the dual gap is zero for this problem. Swapping infimum and supremum will only provide us a lower bound for the minimization problem. Here we hope that we can gain good information from the bound.

$$\inf_{(\rho_i, m_i)_{i \in \{S, I, R\}}} \sup_{(\phi_i)_{i \in \{S, I, R\}}} \mathcal{L}((\rho_i, m_i, \phi_i)_{i \in \{S, I, R\}}) \geq \sup_{\phi_i} \inf_{(\rho_i, m_i)_{i \in \{S, I, R\}}} \mathcal{L}((\rho_i, m_i, \phi_i)_{i \in \{S, I, R\}}).$$

The following propositions are the properties of the saddle point problem derived from optimality conditions (KarushKuhnTucker (KKT) conditions).

**Proposition 1** (Mean field game SIR system). *By KKT conditions, the saddle problem (6) satisfies the following equations.*

$$\left\{ \begin{array}{l} \partial_t \phi_S - \frac{\alpha_S}{2} |\nabla \phi_S|^2 + \frac{\eta_S^2}{2} \Delta \phi_S + c(\rho_S + \rho_I + \rho_R) + \beta(K * (\phi_I \rho_I) - \phi_S K * \rho_I) = 0 \\ \partial_t \phi_I - \frac{\alpha_I}{2} |\nabla \phi_I|^2 + \frac{\eta_I^2}{2} \Delta \phi_I + c(\rho_S + \rho_I + \rho_R) \\ \quad + \beta(\phi_I K * \rho_S - K * (\phi_S \rho_S)) + \gamma \rho(\phi_R - \phi_I) = 0 \\ \partial_t \phi_R - \frac{\alpha_R}{2} |\nabla \phi_R|^2 + \frac{\eta_R^2}{2} \Delta \phi_R + c(\rho_S + \rho_I + \rho_R) = 0 \\ \partial_t \rho_S - \frac{1}{\alpha_S} \nabla \cdot (\rho_S \nabla \phi_S) + \beta \rho_S K * \rho_I - \frac{\eta_S^2}{2} \Delta \rho_S = 0 \\ \partial_t \rho_I - \frac{1}{\alpha_I} \nabla \cdot (\rho_I \nabla \phi_I) - \beta \rho_I K * \rho_S + \gamma \rho_I - \frac{\eta_I^2}{2} \Delta \rho_I = 0 \\ \partial_t \rho_R - \frac{1}{\alpha_R} \nabla \cdot (\rho_R \nabla \phi_R) - \gamma \rho_R - \frac{\eta_R^2}{2} \Delta \rho_R = 0. \end{array} \right. \quad (7)$$

where  $\rho_S(0, \cdot), \rho_I(0, \cdot), \rho_R(0, \cdot)$  are given and

$$\phi_I(T, x) = \delta E(\rho_I(T, x)).$$

*Proof.* By integration by parts, we reformulate the Lagrangian function (6) as follows.

$$\begin{aligned} & L((\rho_i, m_i, \phi_i)_{i \in \{S, I, R\}}) \\ &= E(\rho_I(T, \cdot)) + \int_0^T \int_{\Omega} \beta \phi_I \rho_I K * \rho_S - \beta \phi_S \rho_S K * \rho_I + \gamma \rho_I (\phi_R - \phi_I) dx dt \\ &+ \sum_{i \in \{S, I, R\}} \int_0^T \int_{\Omega} \frac{\alpha_i \|m_i\|^2}{2\rho_i} + \rho_i \partial_t \phi_i + m_i \cdot \nabla \phi_i + \frac{\eta_i^2}{2} \rho_i \Delta \phi_i + \frac{c}{2} (\rho_S + \rho_I + \rho_R)^2 dx dt \\ &+ \sum_{i \in \{S, I, R\}} \int_{\Omega} \rho_i(0, x) \phi_i(0, x) - \rho_i(T, x) \phi_i(T, x) dx \end{aligned}$$

Let the differential of Lagrangian with respect to  $\rho_i, m_i, \phi_i$  ( $i \in \{S, I, R\}$ ),  $\rho_I(T, \cdot)$ , equal to zero. We have

$$\left\{ \begin{array}{l} \frac{\delta}{\delta \rho_i} L = 0 \\ \frac{\delta}{\delta m_i} L = 0 \\ \frac{\delta}{\delta \phi_i} L = 0. \end{array} \right.$$

Hence  $-\nabla \phi_i = \alpha_i \frac{m_i}{\rho_i}$ . And we derive the result.  $\square$

We note that dynamical system (7) models the optimal vector field strategies for S,I,R populations. It combines both strategies from mean field games and SIR models. For this reason, we call (7) *Mean field game SIR system*.

### 3. ALGORITHM

In this section, we implement optimization methods to solve the proposed SIR variational problems. Specifically, we use G-Prox Primal Dual Hybrid Gradient (G-Prox PDHG) method [19]. This is a variation of Chambolle-Pock primal-dual algorithm [8, 9].

**3.1. Review of primal-dual algorithms.** The PDHG method solves the minimization problem

$$\min_x f(Ax) + g(x)$$

by converting it into a saddle point problem

$$\min_x \sup_y \{L(x, y) := \langle Ax, y \rangle + g(x) - f^*(y)\}.$$

Here,  $f$  and  $g$  are convex functions with respect to a variable  $x$ ,  $A$  is a continuous linear operator, and

$$f^*(y) = \sup_x x \cdot y - f(x)$$

is a Legendre transform of  $f$ . For each iteration, the algorithm finds the minimizer  $x_*$  by gradient descent method and the maximizer  $y_*$  by gradient ascent method. Thus, the minimizer and maximizer are calculated by iterating

$$\begin{cases} x^{k+1} &= \arg \min_x L(x, y^k) + \frac{1}{2\tau} \|x - x^k\|^2 \\ y^{k+1} &= \arg \max_y L(x^{k+1}, y) + \frac{1}{2\sigma} \|y - y^k\|^2 \end{cases}$$

where  $\tau$  and  $\sigma$  are step sizes for the algorithm.

Here G-Prox PDHG is a modified version of PDHG that solves the minimization problem by choosing the most appropriate norms for updating  $x$  and  $y$ . Choosing the appropriate norms allows us to choose larger step sizes. Hence, we get a faster convergence rate. In details,

$$\begin{cases} x^{k+1} &= \arg \min_x L(x, y^k) + \frac{1}{2\tau} \|x - x^k\|_{\mathcal{H}}^2 \\ y^{k+1} &= \arg \max_y L(x^{k+1}, y) + \frac{1}{2\sigma} \|y - y^k\|_{\mathcal{G}}^2 \end{cases}$$

where  $\mathcal{H}$  and  $\mathcal{G}$  are some Hilbert spaces with the inner product

$$(u_1, u_2)_{\mathcal{G}} = (Au_1, Au_2)_{\mathcal{H}}.$$

In particular, we use G-Prox PDHG to solve the minimization problem (4) by setting

$$x = (\rho_S, \rho_I, \rho_R, m_S, m_I, m_R), \quad g(x) = F(\rho_i, m_i)_{i \in \{S, I, R\}}, \quad f(Ax) = \begin{cases} 0 & \text{if } Ax = (0, 0, \gamma\rho_I) \\ \infty & \text{otherwise.} \end{cases}$$

$$\begin{aligned} Ax &= (\partial_t \rho_S + \nabla \cdot m_S - \frac{\eta^2}{2} \Delta \rho_S + \beta \rho_S K * \rho_I, \\ &\quad \partial_t \rho_I + \nabla \cdot m_I - \frac{\eta^2}{2} \Delta \rho_I - \beta \rho_I K * \rho_S + \gamma \rho_I, \\ &\quad \partial_t \rho_R + \nabla \cdot m_R - \frac{\eta^2}{2} \Delta \rho_R). \end{aligned}$$

Note that the operator  $A$  is not linear. In the implementation, we approximate the operator with the following linear operator

$$\begin{aligned} Ax &\approx (\partial_t \rho_S + \nabla \cdot m_S - \frac{\eta^2}{2} \Delta \rho_S + \beta \rho_S, \\ &\partial_t \rho_I + \nabla \cdot m_I - \frac{\eta^2}{2} \Delta \rho_I + (\gamma - \beta) \rho_I, \\ &\partial_t \rho_R + \nabla \cdot m_R - \frac{\eta^2}{2} \Delta \rho_R). \end{aligned}$$

**3.2. G-Prox PDHG on SIR variational problem.** In this section, we implement G-Prox PDHG to solve the saddle problem (6). For  $i \in \{S, I, R\}$ ,

$$\begin{aligned} \rho_i^{(k+1)} &= \arg \min_{\rho} \mathcal{L}(\rho, m_i^{(k)}, \phi_i^{(k)}) + \frac{1}{2\tau_i} \|\rho - \rho_i^{(k)}\|_{L^2}^2 \\ m_i^{(k+1)} &= \arg \min_m \mathcal{L}(\rho^{(k+1)}, m, \phi_i^{(k)}) + \frac{1}{2\tau_i} \|m - m_i^{(k)}\|_{L^2}^2 \\ \phi_i^{(k+\frac{1}{2})} &= \arg \max_{\phi} \mathcal{L}(\rho^{(k+1)}, m_i^{(k+1)}, \phi) - \frac{1}{2\sigma_i} \|\phi - \phi_i^{(k)}\|_{H^2}^2 \\ \phi_i^{(k+1)} &= 2\phi_i^{(k+\frac{1}{2})} - \phi_i^{(k)} \end{aligned}$$

where  $\tau_i, \sigma_i$  ( $i \in \{S, I, R\}$ ) are step sizes for the algorithm and by G-Prox PDHG,  $L^2$  norm and  $H^2$  norm are defined as

$$\begin{aligned} \|u\|_{L^2} &= \int_0^T \int_{\Omega} u(t, x)^2 dx dt \\ \|u\|_{H^2} &= \int_0^T \int_{\Omega} (\partial_t u)^2 + \|\nabla u\|^2 + \frac{\eta^4}{4} (\Delta u)^2 dx dt \end{aligned}$$

for any  $u : [0, T] \times \Omega \rightarrow [0, 1]$ .

By formulating these optimality conditions, we can find explicit formulas for each variable.

$$\begin{aligned} \rho_S^{(k+1)} &= \text{root}_+ \left( \frac{\tau_S}{1 + c\tau_S} \left( \partial_t \phi_S^{(k)} + \frac{\eta_S^2}{2} \Delta \phi_S^{(k)} - \frac{1}{\tau_S} \rho_S^{(k)} + \beta \left( K * (\phi_I^{(k)} \rho_I^{(k)}) - \phi_S^{(k)} K * \rho_I^{(k)} \right) \right. \right. \\ &\quad \left. \left. + c(\rho_I + \rho_R) \right), 0, -\frac{\tau_S \alpha_S (m_S^{(k)})^2}{2(1 + c\tau_S)} \right) \\ \rho_I^{(k+1)} &= \text{root}_+ \left( \frac{\tau_I}{1 + c\tau_I} \left( \partial_t \phi_I^{(k)} + \frac{\eta_I^2}{2} \Delta \phi_I^{(k)} - \frac{1}{\tau_I} \rho_I^{(k)} + \beta \left( \phi_I^{(k)} K * \rho_S^{(k)} - K * (\phi_S^{(k)} \rho_S^{(k)}) \right) \right. \right. \\ &\quad \left. \left. + \gamma(\phi_R - \phi_I) + c(\rho_S + \rho_R) \right), 0, -\frac{\tau_I \alpha_I (m_I^{(k)})^2}{2(1 + c\tau_I)} \right) \\ \rho_R^{(k+1)} &= \text{root}_+ \left( \frac{\tau_R}{1 + c\tau_R} \left( \partial_t \phi_R^{(k)} + \frac{\eta_R^2}{2} \Delta \phi_R^{(k)} - \frac{1}{\tau_R} \rho_R^{(k)} + c(\rho_S + \rho_I) \right), 0, -\frac{\tau_R \alpha_R (m_R^{(k)})^2}{2(1 + c\tau_R)} \right) \end{aligned}$$



$$m_i^{(k+1)} = \frac{\rho_i^{(k+1)}}{\tau\alpha_i + \rho_i^{(k+1)}} \left( m_i^{(k)} - \tau \nabla \phi_i^{(k)} \right), \quad (i \in \{S, I, R\})$$

$$\phi_S^{(k+1)} = \phi_S^{(k)} + \sigma_S (A_S^T A_S)^{-1} \left( -\partial_t \rho_S^{(k+1)} - \nabla \cdot m_S^{(k+1)} - \beta \rho_S^{(k+1)} K * \rho_I^{(k+1)} + \frac{\eta_S^2}{2} \Delta \rho_S^{(k+1)} \right)$$

$$\begin{aligned} \phi_I^{(k+\frac{1}{2})} = \phi_I^{(k)} + \sigma_I (A_I^T A_I)^{-1} & \left( -\partial_t \rho_I^{(k+1)} - \nabla \cdot m_I^{(k+1)} + \beta \rho_I^{(k+1)} K * \rho_S^{(k+1)} \right. \\ & \left. - \gamma \rho_I^{(k+1)} + \frac{\eta_I^2}{2} \Delta \rho_I^{(k+1)} \right) \end{aligned}$$

$$\phi_R^{(k+\frac{1}{2})} = \phi_R^{(k)} + \sigma_R (A_R^T A_R)^{-1} \left( -\partial_t \rho_R^{(k+1)} - \nabla \cdot m_R^{(k+1)} + \gamma \rho_I^{(k+1)} + \frac{\eta_R^2}{2} \Delta \rho_R^{(k+1)} \right)$$

where  $root_+(a, b, c)$  is a positive root of a cubic polynomial  $x^3 + ax^2 + bx + c = 0$  and

$$\begin{aligned} A_S^T A_S &= -\partial_{tt} + \frac{\eta_S^4}{4} \Delta^2 - (1 + 2\beta\eta_S)\Delta + \beta^2 \\ A_I^T A_I &= -\partial_{tt} + \frac{\eta_I^4}{4} \Delta^2 - (1 + 2(\gamma - \beta)\eta_S)\Delta + (\gamma - \beta)^2 \\ A_R^T A_R &= -\partial_{tt} + \frac{\eta_R^4}{4} \Delta^2 - \Delta. \end{aligned}$$

We use FFTW library to compute  $(A_i^T A_i)^{-1}$  ( $i \in \{S, I, R\}$ ) by Fast Fourier Transform (FFT). Computing these inverse operators is  $O(n \log n)$  operations per iteration where  $n$  is the number of points. The bottleneck of the algorithm comes from calculating the convolution. Note that the operation can be easily parallelized since the convolution on one point does not affect the convolutions on the other points.

In all, we summarize the algorithm as follows.

---

**Algorithm: G proximal PDHG for mean field game SIR system**

**Input:**  $\rho_i(0, \cdot)$  ( $i \in \{S, I, R\}$ )

**Output:**  $\rho_i, m_i, \phi_i$  ( $i \in \{S, I, R\}$ ) for  $x \in \Omega, t \in [0, T]$

---

**While** relative error  $>$  tolerance

$$\begin{aligned} \rho_i^{(k+1)} &= \arg \min_{\rho} \mathcal{L}(\rho, m_i^{(k)}, \phi_i^{(k)}) + \frac{1}{2\tau_i} \|\rho - \rho_i^{(k)}\|_{L^2}^2 \\ m_i^{(k+1)} &= \arg \min_m \mathcal{L}(\rho^{(k+1)}, m, \phi_i^{(k)}) + \frac{1}{2\tau_i} \|m - m_i^{(k)}\|_{L^2}^2 \\ \phi_i^{(k+\frac{1}{2})} &= \arg \max_{\phi} \mathcal{L}(\rho^{(k+1)}, m_i^{(k+1)}, \phi) - \frac{1}{2\sigma_i} \|\phi - \phi_i^{(k)}\|_{H^2}^2 \\ \phi_i^{(k+1)} &= 2\phi_i^{(k+\frac{1}{2})} - \phi_i^{(k)} \end{aligned}$$

**end**

---

Here, the relative error is defined as

$$\text{relative error} = \frac{|P(\rho_i^{(k+1)}, m_i^{(k+1)}) - P(\rho_i^{(k)}, m_i^{(k)})|}{|P(\rho_i^{(k)}, m_i^{(k)})|}.$$

#### 4. EXPERIMENTS

In this section, we present two sets of numerical experiments using the algorithm with various parameters and all algorithms are coded in C++. Let  $\Omega = [0, 1]^2$  be a unit cube in  $\mathbb{R}^2$  and  $T = 1$ . The domain  $\Omega$  is discretized with the regular rectangular mesh

$$x_{kl} = \left( \frac{k + 0.5}{N_x}, \frac{l + 0.5}{N_y} \right), \quad k = 0, \dots, N_x - 1, \quad l = 0, \dots, N_y - 1$$

$$t_n = \frac{n}{N_t - 1}, \quad n = 0, \dots, N_t - 1.$$

where  $N_x, N_y$  are the number of data points in space and  $N_t$  is the number of data points in time. For all the experiments, we use the same set of parameters,

$$N_x = 128, \quad N_y = 128, \quad N_t = 32$$

$$\sigma = 0.01, \quad c = 0.01 \quad \beta = 0.7, \quad \eta_i = 0.01 \quad (i \in \{S, I, R\})$$

$$\alpha_S = 1, \quad \alpha_I = 10, \quad \alpha_R = 1$$

and a terminal cost functional

$$E(\rho_I(1, \cdot)) = \frac{1}{2} \int_{\Omega} \rho_I^2(1, x) dx.$$

By setting higher value for  $\alpha_I$ , we penalize the movement of infected population more than other populations. Considering the immobility of infected individuals, this is a reasonable choice in terms of real-world applications.

To minimize the terminal cost functional  $E(\rho_I)$ , a solution needs to minimize the number of infected population. There are mainly two ways of reducing the number of infected. First way is to transition infected to recovered population. However, it may not be feasible if a rate of recovery  $\gamma$  is small. Another way to reduce the number of infected is by separating susceptible population from infected population. The number of infected doesn't increase if there are no susceptible people near infected. However, the total cost increases when densities move due to  $\rho_i \|v_i\|^2$  ( $i \in \{S, I, R\}$ ) terms in the running cost. A solution needs to find the optimal balance between the terminal cost and the running cost. The following two sets of experiments show that the algorithm finds the proper solutions based on values of  $\gamma$  given different initial densities.

**4.1. Experiment 1.** In this experiment, initial densities for susceptible, infected, and recovered populations are

$$\rho_S(0, x) = 0.5 \exp\left(-10((x_1 - 0.5)^2 + (x_2 - 0.5)^2)\right)$$

$$\rho_I(0, x) = 15(0.03 - (x_1 - 0.6)^2 - (x_2 - 0.6)^2)_+$$

$$\rho_R(0, x) = 0$$

where

$$(x)_+ = \begin{cases} x & \text{if } x > 0 \\ 0 & \text{otherwise.} \end{cases}$$

Susceptible population is a Gaussian distribution centered at  $(0.5, 0.5)$  and infected population is concentrated at  $(0.6, 0.6)$ .

We show two different numerical results with a low rate of recovery  $\gamma = 0.1$  (Figure 1) and a high rate of recovery  $\gamma = 0.5$  (Figure 2). In both figures, the evolution of densities  $\rho_i$  ( $i \in \{S, I, R\}$ ) are shown at  $t = 0, 0.21, 0.47, 0.74, 1$ . The total population of each density is indicated as sum in the subtitle of each plot.

When  $\gamma$  is small (Figure 1), the solution separates susceptible population from infected population. By separating susceptible from infected, the solution minimizes the terminal cost at  $t = 1$ . When  $\gamma$  is large (Figure 2), susceptible population barely moves over time. The solution minimizes the terminal cost by converting infected to recovered population which is considered to be cheaper than moving susceptible away from infected.

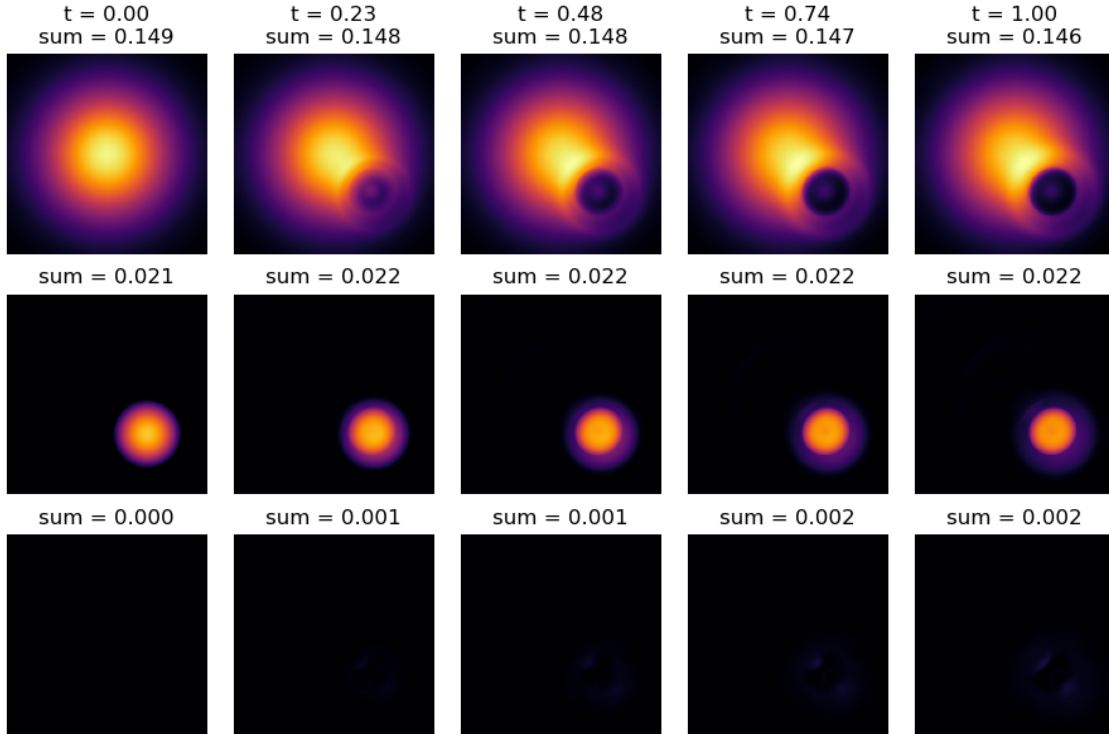


FIGURE 1. Experiment 1. The evolution of populations from  $t = 0$  to  $t = 1$  with  $\beta = 0.7$  and  $\gamma = 0.1$ . The first row represents susceptible, the second row represents infected, and the last row represents recovered. The solution moves susceptible away from the infected over time.

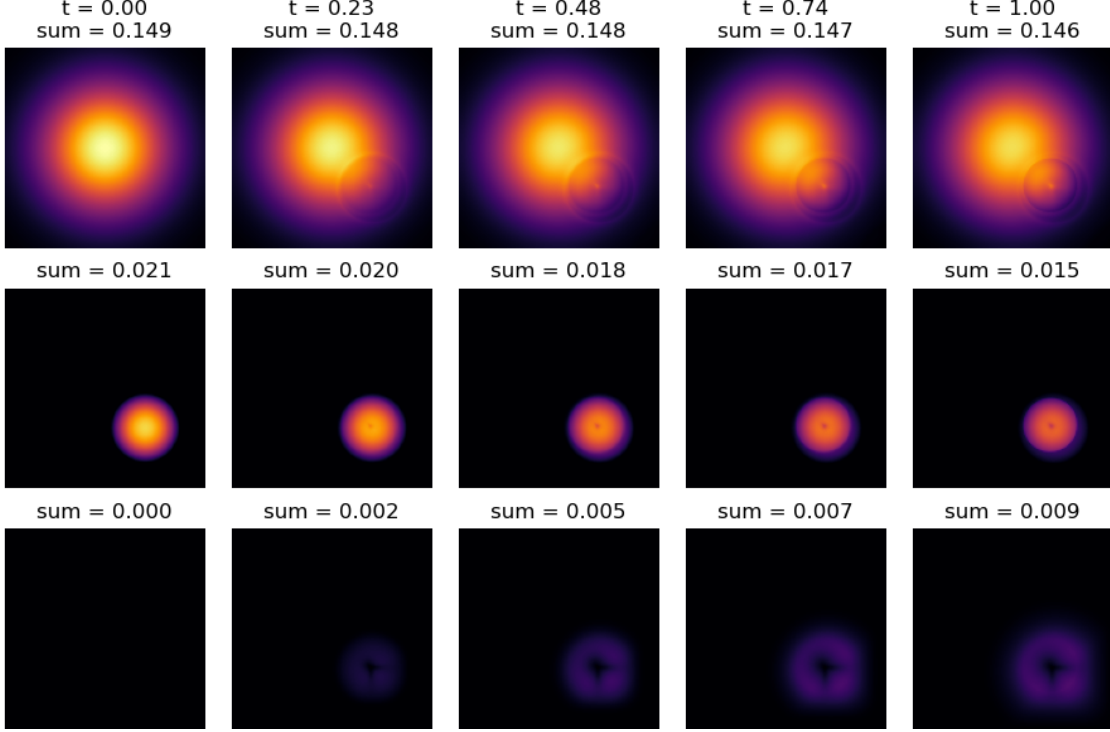


FIGURE 2. Experiment 1. The evolution of populations from  $t = 0$  to  $t = 1$  with  $\beta = 0.7$  and  $\gamma = 0.5$ . The first row represents susceptible, the second row represents infected, and the last row represents recovered. The solution minimizes the number of infected at time  $t = 1$  by recovering infected population.

4.2. **Experiment 2.** In this experiment, initial densities for susceptible, infected, and recovered populations are

$$\begin{aligned}\rho_S(0, x) &= 0.5 \\ \rho_I(0, x) &= 70 \left( 0.005 - \left( \sqrt{(x-0.5)^2 + (y-0.5)^2} - 0.25 \right)^2 \right)_+ \\ \rho_R(0, x) &= 0.\end{aligned}$$

Susceptible population is a uniform distribution on  $\Omega$  and infected population is a ring shaped density centered at  $(0.5, 0.5)$ . We again show that two different numerical results with a low rate of recovery  $\gamma = 0.1$  (Figure 3) and a high rate of recovery  $\gamma = 0.5$  (Figure 4). Similar to Experiment 1, we see that the solution minimizes the number of infection by moving susceptible away from infected when  $\gamma$  is small. By separating these two populations, it minimizes the rate of contacts between susceptible and infected. When  $\gamma$  is large, the solution converts infected to recovered population rather than moving susceptible population.

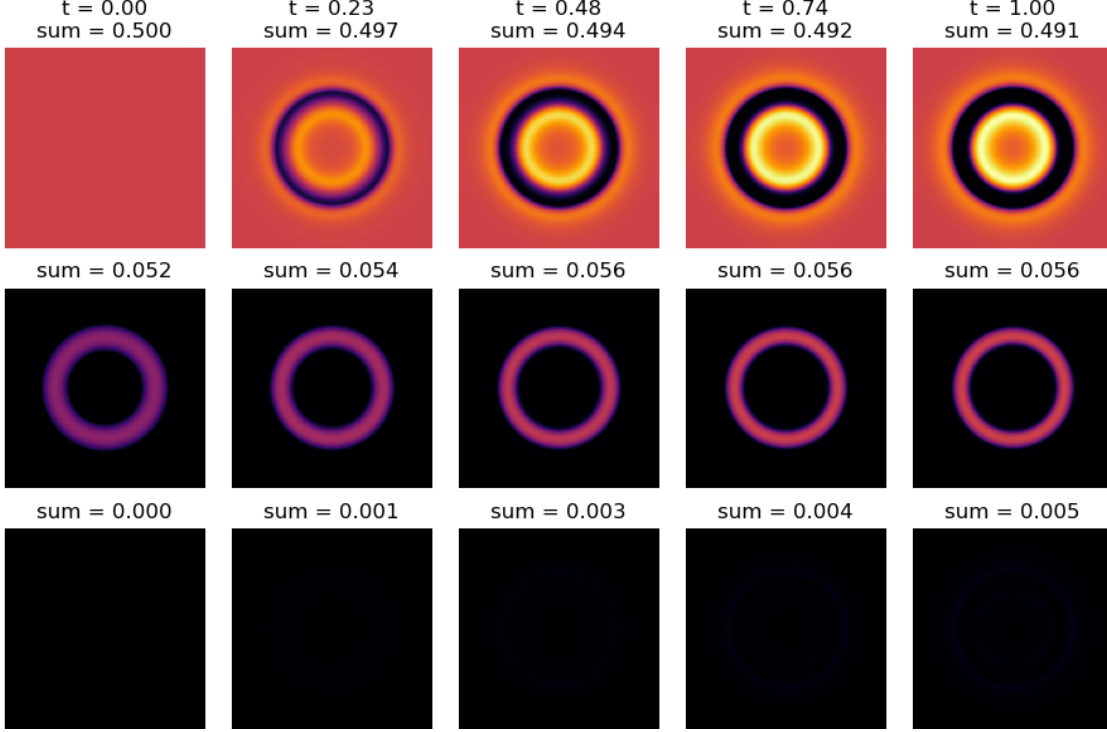


FIGURE 3. Experiment 2. The evolution of populations from  $t = 0$  to  $t = 1$  with  $\beta = 0.7$  and  $\gamma = 0.1$ . The first row represents susceptible, the second row represents infected, and the last row represents recovered.

4.3. **Experiment 3.** In this experiment, we consider nonsymmetric initial densities.

$$\begin{aligned}
 \rho_S(0, x) &= 0.45 \left( \exp(-15((x - 0.3)^2 + (y - 0.3)^2)) \right. \\
 &\quad + \exp(-25((x - 0.5)^2 + (y - 0.75)^2)) \\
 &\quad \left. + \exp(-30((x - 0.8)^2 + (y - 0.35)^2)) \right) \\
 \rho_I(0, x) &= 10(0.04 - (x - 0.2)^2 - (y - 0.65)^2)_+ \\
 &\quad + 12(0.03 - (x - 0.5)^2 - (y - 0.2)^2)_+ \\
 &\quad + 12(0.03 - (x - 0.8)^2 - (y - 0.55)^2)_+ \\
 \rho_R(0, x) &= 0.
 \end{aligned}$$

Susceptible population is the sum of three Gaussian distributions and infected population is the sum of positive part of quadratic polynomials. We conduct this experiment to show that the algorithm works for nonsymmetric initial densities. Using the same set of parameters, the experiment is repeated twice with  $\gamma = 0.1$  and  $\gamma = 0.5$ . The same behavior of solutions can be observed from Figure 5 and Figure 6.

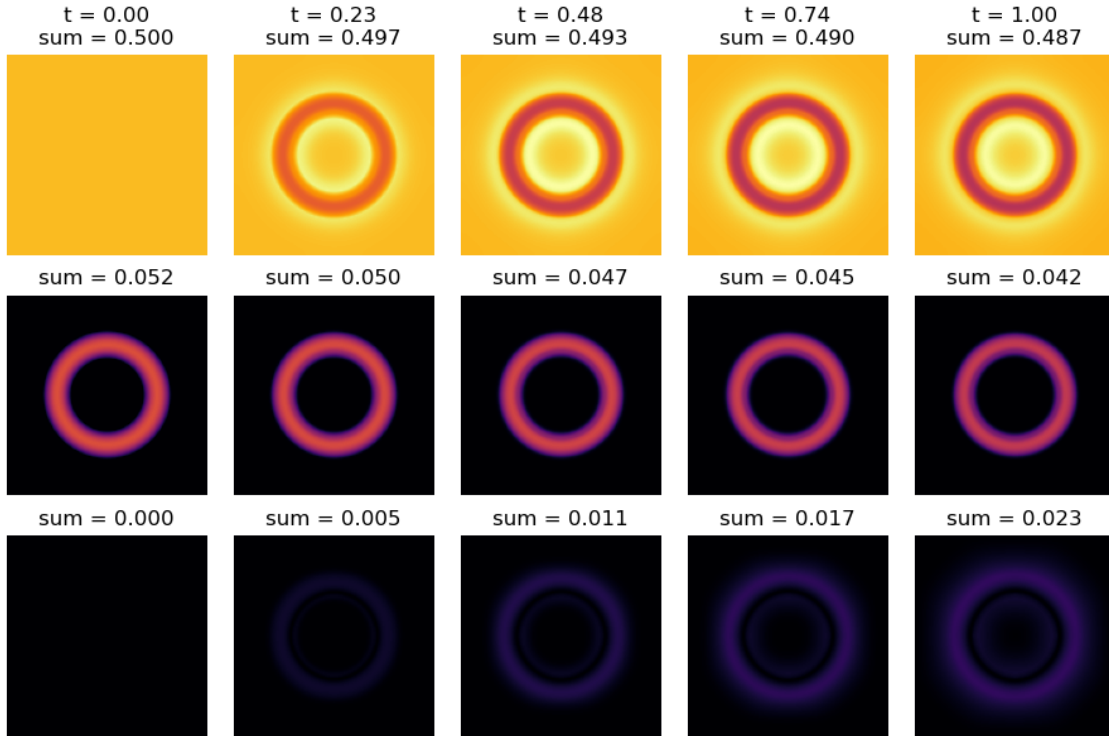


FIGURE 4. Experiment 2. The evolution of populations from  $t = 0$  to  $t = 1$  with  $\beta = 0.7$  and  $\gamma = 0.5$ . The first row represents susceptible, the second row represents infected, and the last row represents recovered.

## 5. DISCUSSION

In this paper, we introduce a mean-field game model for controlling the virus spreading of a population in a spatial domain, which extends and controls the current SIR model with spatial effect. Here the state variable represents the population status, such as S, I, R, etc with a spatial domain, while the control variable is the velocity of motion of the population. The terminal cost forms the goal of government, which balances the total infection number and maintain suitable physical movement of essential tasks and goods. Numerical algorithms are derived to solve the proposed model. Several experiments demonstrate that our model can effectively demonstrate how to separate the infected and susceptible population in a spatial domain.

Our model opens the door to many questions in modeling, inverse problems and computations, especially during this COVID-19 pandemic. On the modeling side, first, we are interested in generalize the geometry of the spatial domain. Second, our current model only focuses on the control of population movement. The control of the diffusion operator among populations is also of great interests in future work. Third, the government can also put restrictions on the interaction for different class of populations, depending on their infection status. Fourth, in real life, the spatial domain is often inhomogeneous, containing airports, schools, subways etc. We also need to formulate our mean-field game model on a

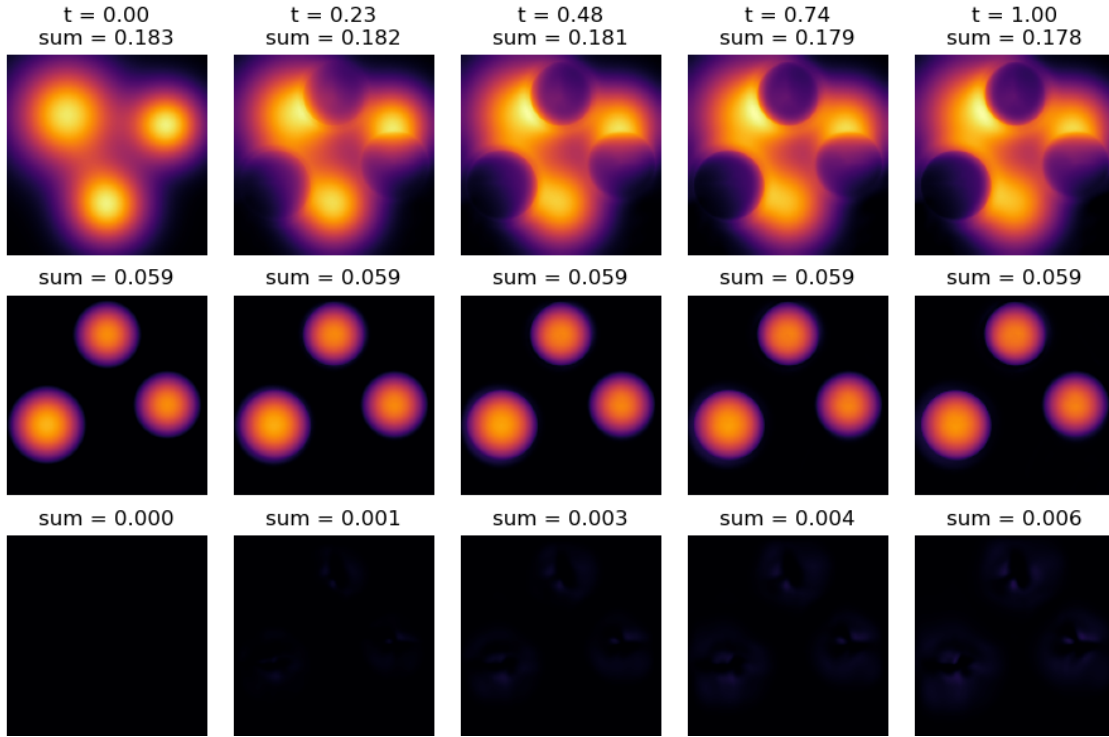


FIGURE 5. Experiment 3. The evolution of populations from  $t = 0$  to  $t = 1$  with  $\beta = 0.7$  and  $\gamma = 0.1$ . The first row represents susceptible, the second row represents infected, and the last row represents recovered.

discrete spatial graph (network). In addition, our model focus on the forward problem of modeling the dynamics of the virus. In practice, real time data is generated as the virus spreading across different regions. To effectively model this dynamic, a suitable inverse mean-field game problem needs to be constructed. On the computational side, our model involves a non-convex optimization problem, which comes from the multiplicative term of the SIR model itself. In future work, we expect to design a fast and reliable algorithm for these advanced models. We also expect to develop and apply AI numerical algorithms to compute models in high dimensions.

#### REFERENCES

- [1] Yves Achdou and Jean-Michel Lasry. Mean field games for modeling crowd motion. In *Contributions to partial differential equations and applications*, volume 47 of *Comput. Methods Appl. Sci.*, pages 17–42. Springer, Cham, 2019.
- [2] DG Aronson. The asymptotic speed of propagation of a simple epidemic. In *Nonlinear diffusion*, volume 14, pages 1–23. Pitman London, 1977.
- [3] J.-D. Benamou and G. Carlier. Augmented Lagrangian methods for transport optimization, mean field games and degenerate elliptic equations. *J. Optim. Theory Appl.*, 167(1):1–26, 2015.
- [4] Henri Berestycki, Jean-Michel Roquejoffre, and Luca Rossi. Propagation of epidemics along lines with fast diffusion. *arXiv preprint arXiv:2005.01859*, 2020.

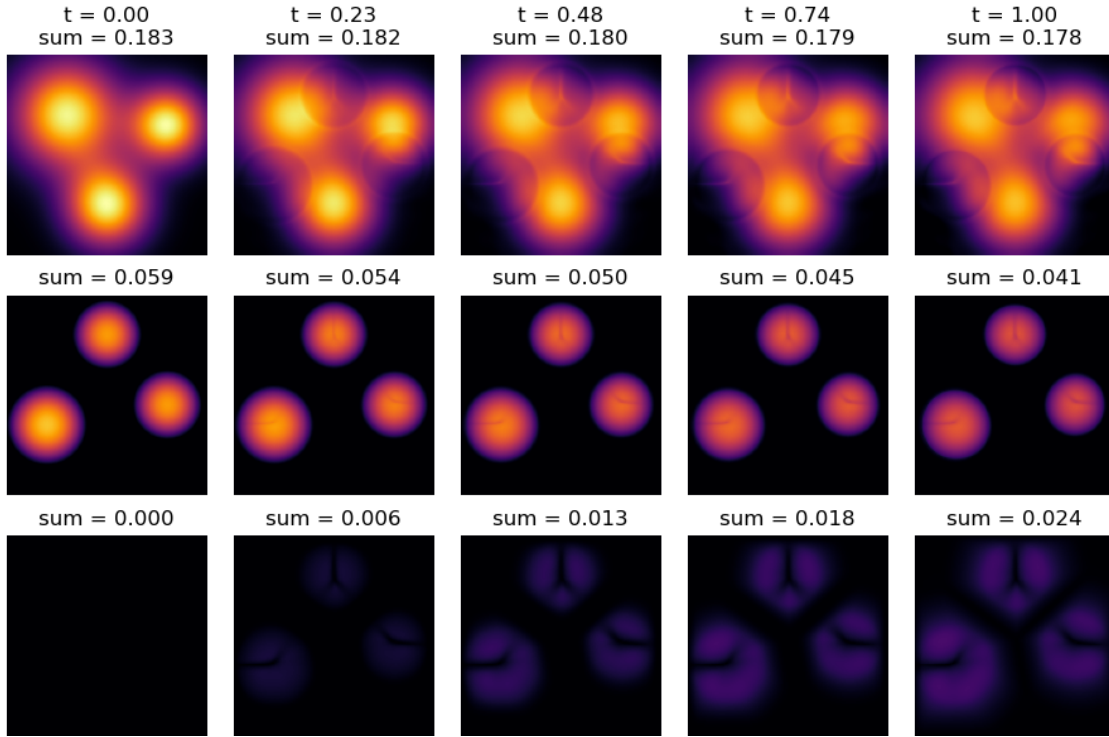


FIGURE 6. Experiment 3. The evolution of populations from  $t = 0$  to  $t = 1$  with  $\beta = 0.7$  and  $\gamma = 0.5$ . The first row represents susceptible, the second row represents infected, and the last row represents recovered.

- [5] L. M. Briceño Arias, D. Kalise, and F. J. Silva. Proximal methods for stationary mean field games with local couplings. *SIAM J. Control Optim.*, 56(2):801–836, 2018.
- [6] Martin Burger, Marco Di Francesco, Peter Markowich, and Marie-Therese Wolfram. Mean field games with nonlinear mobilities in pedestrian dynamics. *arXiv preprint arXiv:1304.5201*, 2013.
- [7] Thomas Caraco, Stephan Glavanakov, Gang Chen, Joseph E Flaherty, Toshiro K Ohsumi, and Boleslaw K Szymanski. Stage-structured infection transmission and a spatial epidemic: a model for lyme disease. *The American Naturalist*, 160(3):348–359, 2002.
- [8] Antonin Chambolle and Thomas Pock. A first-order primal-dual algorithm for convex problems with applications to imaging. *J. Math. Imaging Vision*, 40(1):120–145, 2011.
- [9] Antonin Chambolle and Thomas Pock. On the ergodic convergence rates of a first-order primal-dual algorithm. *Math. Program.*, 159(1-2, Ser. A):253–287, 2016.
- [10] Setthapat Chinviriyasit and Wirawan Chinviriyasit. Numerical modelling of an sir epidemic model with diffusion. *Applied Mathematics and Computation*, 216(2):395–409, 2010.
- [11] Odo Diekmann. Run for your life. a note on the asymptotic speed of propagation of an epidemic. *Journal of Differential Equations*, 33(1):58–73, 1979.
- [12] Weinan E, Jiequn Han, and Qianxiao Li. A Mean-Field Optimal Control Formulation of Deep Learning. *arXiv:1807.01083 [cs, math]*, 2018.
- [13] István Faragó and Róbert Horváth. Qualitatively adequate numerical modelling of spatial sirs-type disease propagation. *Electronic Journal of Qualitative Theory of Differential Equations*, 2016(12):1–14, 2016.
- [14] Diogo A Gomes et al. Mean field games models: a brief survey. *Dynamic Games and Applications*, 4(2):110–154, 2014.



- [15] Diogo A Gomes, Levon Nurbekyan, and Edgard A Pimentel. *Economic models and mean-field games theory*. IMPA Mathematical Publications. Instituto Nacional de Matemática Pura e Aplicada (IMPA), Rio de Janeiro, 2015.
- [16] Bryan T Grenfell, Ottar N Björnstad, and Jens Kappey. Travelling waves and spatial hierarchies in measles epidemics. *Nature*, 414(6865):716–723, 2001.
- [17] Yuzo Hosono and Bilal Ilyas. Traveling waves for a simple diffusive epidemic model. *Mathematical Models and Methods in Applied Sciences*, 5(07):935–966, 1995.
- [18] M. Huang, R. P. Malhamé, and P. E. Caines. Large population stochastic dynamic games: closed-loop McKean-Vlasov systems and the Nash certainty equivalence principle. *Commun. Inf. Syst.*, 6(3):221–251, 2006.
- [19] Matt Jacobs, Flavien Léger, Wuchen Li, and Stanley Osher. Solving Large-Scale Optimization Problems with a Convergence Rate Independent of Grid Size. *arXiv:1805.09453 [math]*, 2018.
- [20] Atit Jaichuang and Wirawan Chinviriyasit. Numerical modelling of influenza model with diffusion. *International Journal of Applied Physics and Mathematics*, 4(1):15, 2014.
- [21] Junyoung Jang, Hee-Dae Kwon, and Jeehyun Lee. Optimal control problem of an sir reaction–diffusion model with inequality constraints. *Mathematics and Computers in Simulation*, 171:136–151, 2020.
- [22] Boyan Jovanovic and Robert W. Rosenthal. Anonymous sequential games. *Journal of Mathematical Economics*, 17(1):77 – 87, 1988.
- [23] Anders Källén. Thresholds and travelling waves in an epidemic model for rabies. *Nonlinear Analysis: Theory, Methods & Applications*, 8(8):851–856, 1984.
- [24] David G Kendall. Mathematical models of the spread of infection. *Mathematics and computer science in biology and medicine*, pages 213–225, 1965.
- [25] William Ogilvy Kermack and Anderson G McKendrick. A contribution to the mathematical theory of epidemics. *Proceedings of the royal society of london. Series A, Containing papers of a mathematical and physical character*, 115(772):700–721, 1927.
- [26] Aimé Lachapelle, Jean-Michel Lasry, Charles-Albert Lehalle, and Pierre-Louis Lions. Efficiency of the price formation process in presence of high frequency participants: a mean field game analysis. *Mathematics and Financial Economics*, 10(3):223–262, 2016.
- [27] A Lahrouz, H El Mahjour, A Settati, and A Bernoussi. Dynamics and optimal control of a nonlinear epidemic model with relapse and cure. *Physica A: Statistical Mechanics and its Applications*, 496:299–317, 2018.
- [28] Jean-Michel Lasry and Pierre-Louis Lions. Jeux à champ moyen. I. Le cas stationnaire. *C. R. Math. Acad. Sci. Paris*, 343(9):619–625, 2006.
- [29] Jean-Michel Lasry and Pierre-Louis Lions. Jeux à champ moyen. II. Horizon fini et contrôle optimal. *C. R. Math. Acad. Sci. Paris*, 343(10):679–684, 2006.
- [30] Jean-Michel Lasry and Pierre-Louis Lions. Mean field games. *Japanese journal of mathematics*, 2(1):229–260, 2007.
- [31] Kezan Li, Guanghu Zhu, Zhongjun Ma, and Lijuan Chen. Dynamic stability of an siqs epidemic network and its optimal control. *Communications in Nonlinear Science and Numerical Simulation*, 66:84–95, 2019.
- [32] Alex Tong Lin, Samy Wu Fung, Wuchen Li, Levon Nurbekyan, and Stanley J. Osher. Apac-net: Alternating the population and agent control via two neural networks to solve high-dimensional stochastic mean field games, 2020.
- [33] Siting Liu, Matthew Jacobs, Wuchen Li, Levon Nurbekyan, and Stanley J Osher. Computational methods for nonlocal mean field games with applications. *arXiv preprint arXiv:2004.12210*, 2020.
- [34] JD Murray. *Mathematical biology II: spatial models and biomedical applications*. Springer New York, 2001.
- [35] Shigui Ruan. Spatial-temporal dynamics in nonlocal epidemiological models. In *Mathematics for life science and medicine*, pages 97–122. Springer, 2007.
- [36] Lars Ruthotto, Stanley Osher, Wuchen Li, Levon Nurbekyan, and Samy Wu Fung. A machine learning framework for solving high-dimensional mean field game and mean field control problems, 2019.
- [37] Suresh P Sethi and Preston W Staats. Optimal control of some simple deterministic epidemic models. *Journal of the Operational Research Society*, 29(2):129–136, 1978.

- [38] HR Thieme. A model for the spatial spread of an epidemic. *Journal of Mathematical Biology*, 4(4):337–351, 1977.
- [39] Zhi-Cheng Wang and Jianhong Wu. Travelling waves of a diffusive kermack–mckendrick epidemic model with non-local delayed transmission. *Proceedings of the Royal Society A: Mathematical, Physical and Engineering Sciences*, 466(2113):237–261, 2010.